2025-01-8451

Effects of Critical Compression Ratio on Rating Gasoline Knock Propensity

Author, co-author (Do NOT enter this information. It will be pulled from participant tab in MyTechZone)

Affiliation (Do NOT enter this information. It will be pulled from participant tab in MyTechZone)

Abstract

It is common practice in the automotive industry to explore the knock limits of fuels on an engine by a comparison of the knock limited spark advance (KLSA) at threshold knock intensity. However, the knock propensity of gasolines can be rated by changing one of three metrics on a variable compression ratio Cooperative Fuels Research (CFR) octane rating engine while holding the other two variables constant: knock intensity, spark timing, and critical compression ratio. The operational differences between the standard research octane number (RON) rating and modern engine operation have been explored in three parts. The first part focused on the effects of lambda and knock characterization. The second part studied the effects of spark timing. This third part explores the knock ratings of several gasolines by comparing the critical compression ratios at constant combustion phasing and knock intensity. The threshold knock intensity was based on the standard octane rating D1 pickup or by maximum amplitude of pressure oscillations (MAPO) measured by a piezoelectric cylinder pressure transducer. Several Fuels for Advanced Combustion Engines (FACE) gasolines, primary reference fuels (PRFs), and toluene standardization fuels (TSFs) were tested on a CFR octane rating engine with advanced data acquisition equipment and a piezoelectric cylinder pressure transducer. These tests deviated from the ASTM D2699 standard octane rating procedure. For each test fuel, the CFR engine was operated at stoichiometry at a constant combustion phasing (CA50) and the compression ratio was modified until a threshold knock intensity was realized. It was found that the chemical composition of the fuels affected the relationship of critical compression ratios between the D1 knockmeter and piezoelectric pressure transducer knock intensity thresholds, as well as the measured combustion maximum pressure rise rate and spark timing setting for constant CA50. For highly aromatic fuels tested at a constant MAPO knock intensity threshold, it was found that the maximum pressure rise rate was two to three times higher than that of highly paraffinic fuels with similar RON and the spark advance was several crank angle degrees less for constant combustion phasing.

Introduction

Today's carbon dioxide (CO_2) emissions targets for internal combustion engines are regulated by most governments worldwide [1,2]. Spark ignition (SI) engines usually improve efficiency and performance by increasing compression ratio, down-speeding, and downsizing in combination with turbocharging, allowing the engine to operate in a more efficient part of the operating map, resulting in lower vehicle fuel consumption.

End gas autoignition in the combustion chamber during propagating flame (spark-ignited) combustion is governed by the time an air-fuel mixture spends at a given pressure and temperature. Autoignition of the air-fuel mixture causes multiple flame fronts with local high heat release rates within the combustion chamber, subsequently creating superimposed high-frequency pressure oscillations called "knock". Knocking combustion can damage the materials of the combustion chamber and therefore limits are imposed on the performance and efficiency of a spark-ignited internal combustion engine to avoid knock.

The standard measurements of knock resistance of gasoline are the Research and Motor Octane Numbers (RON, MON). The RON and MON ratings are performed on a Cooperative Fuels Research (CFR) engine at defined operating conditions following ASTM D2699 and D2700 methods, respectively [3, 4]. Table 1 summarizes the operating conditions of RON and MON while Table 2 provides important engine parameters of the CFR engine. The CFR engine is a single-cylinder internal combustion engine designed to withstand harsh knocking combustion and is equipped with a unique variable compression ratio system that allows continuous compression ratio adjustment even while the engine is firing or knocking. The CFR engine is operated under naturally aspirated conditions. The RON test is conducted at lower engine speeds and intake air temperatures compared to MON [3, 4].

Table 1 Overview of operating conditions for RON and MON ratings [3, 4]

Parameter	**RON**	**MON**
Engine Speed	600 RPM	900 RPM
Intake Air Temperature	52 °C	38 °C
Mixture Air Temperature	Not controlled	149 °C
Spark Timing	13 °bTDC	Variable, depending on compression ratio
Lambda	Maximum Knock	Maximum Knock
Intake Pressure	Naturally aspirated, wide open throttle	Naturally aspirated, wide open throttle
Compression Ratio	Based on octane level and barometric pressure	Based on octane level and barometric pressure

Table 2. Overview of CFR Engine geometric parameters [3, 4]

Parameter	CFR Engine
Displacement	0.612 liters
Cylinder Bore	8.255 cm
Stroke	11.43 cm
Compression Ratio	Continuously variable from 4:1 to 18:1
Fuel System	Carbureted with four fuel bowls
Intake Valve	One shrouded non-rotating valve
Exhaust Valve	One non-shrouded rotating valve
Valve Overlap	5 CAD
Combustion Chamber Geometry	Pancake
Spark Plug	Side-mounted

The CFR engine, along with the RON and MON methods, were developed in the early 1930s and therefore differ somewhat from modern engine operation [5-8]. In 1932, MON had a superior correlation to on-road fuel performance. Advances in engine technology such as better engine cooling systems shifted the relevance to RON [9]. For this reason, the current study will focus on the RON test method. In 2001, Kalghatgi introduced the Octane Index (OI), which established a linear trendline with RON and MON as boundaries, equation 1 [10]. The Octane Index generates superior correlations of fuel knock resistance with modern engines over RON and MON due to the engine operation-specific factor K, which represents the slope between RON (K=0) and MON (K=1).

$$OI = RON - K * (RON - MON) \quad (1)\ [10]$$

Mittal et al. investigated the evolution of the K-factor distribution and showed that historically, engines had a K-factor around 0.5, which would equate to the average of RON and MON and is termed the anti-knock index (AKI) [9]. The anti-knock index is used as the most common fuel rating for commercial gasoline sales in the United States. Mittal et al. also showed that naturally aspirated spark-ignited engines from the 2008 timeframe had a K value close to 0, meaning RON was more representative than MON. Furthermore, spark ignition engines with forced induction tended toward negative K-factors, around -0.5 [9].

Over the last several years, the authors and others have investigated the standard RON rating method in greater detail through applying modern engine research instrumentation to the standard CFR octane rating engine to better understand how the RON rating conditions compare and contrast to knock assessments in modern automotive SI engines [11-18]. After reviewing previous work, it was determined that there was a need for further detailed combustion measurements on the CFR engine under standard RON rating conditions, as well as operating conditions mimicking modern SI engine operation. This work carries previous work in this area one step further by examining 12 test fuels with specific variations to their chemical compositions, using legacy and modern knock detection methods, and applying the variable compression ratio mechanism of the CFR engine as a key test parameter.

Methodology

There is a triangular relationship between knock intensity, spark timing, and compression ratio (CR), Figure 1. Two of the listed parameters can remain constant while the third parameter can be used to rate the fuel's knock resistance. The first paper of a three-part publication series focused on the effects of lambda and knock intensity (KI) characterization, while retaining a constant spark timing and compression ratio [15]. The second publication studied the effects of spark timing and combustion phasing while retaining a constant knock intensity and compression ratio, [16]. This paper is the third and final part of this knock propensity evaluation across the triangular relationship in Figure 1. This paper targets testing a matrix of fuels at constant combustion phasing and knock intensity by varying the compression ratio as a means of using the compression ratio as the knock rating metric.

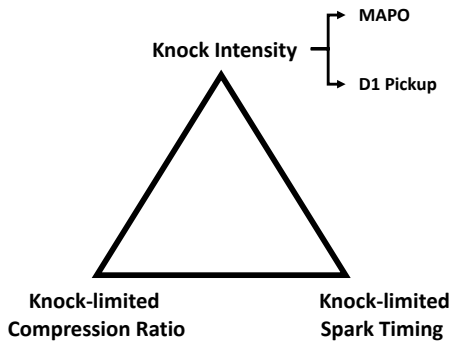

Figure 1. Knock rating triangle. One parameter to be used for knock evaluation while remaining two parameters are kept constant. Note that in this work the knock intensities and spark timing is held constant, while varying the knock-limited compression ratio.

Every CFR engine has a continuously variable compression ratio while the engine is operating by adjusting the height of the cylinder and cylinder head, and therefore modifying the clearance volume. Procedure C of the standard RON test method utilizes this variable compression ratio mechanism to rate the RON of fuels while keeping a constant knock intensity with the knockmeter [3]. In this method, a knock threshold is determined by using octane reference fuels. The sample fuel is then operated, and the compression ratio is varied until the threshold knock limit is achieved. Higher critical CR at a given knock threshold equates to a more knock resistant fuel. This study utilizes the varying compression ratio to match a threshold knock intensity, similar to Procedure C, but also explores adjustments to the fuel-air ratio, spark-timing, and knock intensity characterization technique.

Experimental Procedures

All experiments were conducted on a CFR engine. Before any engine upgrades were performed, the engine passed the motoring peak pressure test and Fit for Use requirements based on the ASTM RON method [3]. For standard octane tests, the knock intensity of a sample fuel is compared relative to primary reference fuels (PRF). PRFs are a binary blend of iso-octane and n-heptane, with a defined octane number equal to the volumetric percentage of iso-octane. The knock intensity during a standard octane test is characterized by a standardized knockmeter system, which consists of a D1 Detonation Pickup, a 501C Detonation Meter, and a knockmeter scale [3]. A piezoelectric pressure transducer was employed to simultaneously measure the maximum amplitude of pressure oscillations (MAPO) knock intensity as well. Figure 2 shows a representative knocking pressure trace for PRF98 (blue) measured on the CFR engine used in this study. The orange line (right y-axis) shows the resultant pressure

data after applying a band pass filtered and rectifying the signal. The MAPO knock intensity for each combustion cycle was defined as the maximum value of the band pass and rectified cylinder pressure data. All data points were collected at steady-state operation for 300 consecutive cycles. The cylinder pressure data (e.g., MAPO, maximum pressure rise rate, etc.) was calculated for each of the 300 cycles and then averaged.

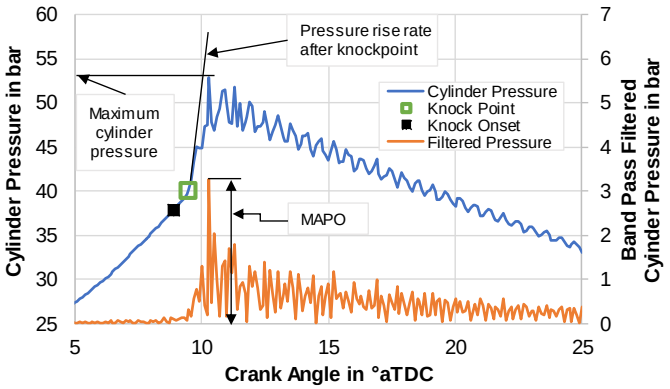

Figure 2. Representative cylinder pressure trace for PRF98 at PKL presented as a function of crank angle, highlighting Knock Onset and Knock Point.

For each fuel, a multi-step test procedure was conducted. One gasoline of the fuel matrix (FACE-G) was selected as an example in the following explanation since it showed the overall lowest MAPO knock intensity in the previous work. Therefore, all other FACE gasolines should require a lower MAPO-based critical CR relative to FACE-G. At first, each fuel was tested under standard RON conditions following the ASTM RON test method [3]. The only deviation from the standard RON test method was the utilization of building compressed air to supply the intake air of the engine since it allows for tighter control of the intake air pressure and relative humidity than using ambient air. For these tests, an intake pressure of 1.0 bara was selected. During standard RON testing at the D2699 compression ratio, peak knocking lambda, and standard spark timing, the knockmeter knock intensity for each fuel was recorded. Column two of Table 3 shows key testing parameters of this standard RON test for FACE-G. In the second step, the lambda was shifted to a stoichiometric air-to-fuel ratio at otherwise constant operating conditions, cf. column three of Table 3. The shift from a rich to a stoichiometric air-to-fuel ratio reduced the knockmeter and MAPO knock intensities, decreased the indicated mean effective pressure (IMEP), and delayed the CA50. For FACE-G, the CA50 at stoichiometric conditions was 11.7°aTDC. In the next tests, the compression ratio was increased to raise the knock intensity back to the desired knock threshold, based either on the knockmeter or MAPO. Subsequently, the compression ratio represents the knock rating of the fuels during this experimental study. In the case of the knockmeter, the targeted knock intensity was that from the first test at standard RON conditions which is, except for the stoichiometric air-to-fuel ratio, identical to Procedure C of the standard RON test. For the MAPO knock intensity, a constant knock intensity threshold of 0.6 bar was defined. The changes in compression ratio and air-to-fuel ratio impacted the combustion phasing of the fuel. To enable a consistent rating across fuels, the spark timing for all fuels was adjusted for a constant CA50 at 12°aTDC, which was close to the stoichiometric operation of FACE-G. Furthermore, a constant IMEP was also targeted for these tests by minimally adjusting the intake manifold pressure setpoint up to ±0.005 bara utilizing the compressed air intake system. Columns four and five of Table 3 show the respective operating conditions for the variable compression ratio tests with either constant knockmeter or constant MAPO knock intensity. Table 4 clarifies the engine test conditions that were targeted to be held constant for the tests described in columns four and five of Table 3.

The variable compression ratio rating method of this study first shifted operating conditions from standard RON conditions to stoichiometric RON and then increased the compression ratio to raise the knock intensity to the desired threshold, 0.6 bar MAPO or 27 ±1 KI knockmeter. Subsequently, almost every cycle of this study is expected to be knocking for each fuel tested.

Table 3. Example of testing methodology for the variable compression ratio testing for FACE-G gasoline.

Parameter	Std. RON	Stoich. RON	Knockmeter Threshold	MAPO Threshold
Compression Ratio	7.26:1	7.26:1	7.31:1	7.88:1
Spark Timing	-13°aTDC	-13°aTDC	-12.4°aTDC	-10.8°aTDC
CA50	10.3°aTDC	11.7°aTDC	12.1°aTDC	11.8°aTDC
Lambda	0.95	1.00	1.00	1.01
IMEP	7.7 bar	7.6 bar	7.6 bar	7.6 bar
Knockmeter	27	22	26	86
MAPO	0.33 bar	0.31 bar	0.33 bar	0.6 bar

Table 4. Fixed operating conditions during fuels test matrix.

Engine Speed	600 RPM
Intake Pressure	1.0 ±0.005 bara
Intake Temperature	52 °C
Coolant Temperature	100 °C
Target CA50	12 °aTDC
IMEP	7.6 bar
Knock Threshold	MAPO: 0.6 bar Knockmeter: Based on RON rating.

CFR Engine Upgrades

A standard CFR F-1 octane rating engine was upgraded to allow for more detailed measurements of engine operation, combustion, and knock. The engine was outfitted with a LabVIEW-based data acquisition system to monitor temperatures, pressures, and relative humidity throughout the intake and exhaust system. The engine was also outfitted with modern combustion research tools such as a wide-band lambda sensor and a spark plug cylinder pressure transducer. Table 5 and previous publications provide a more detailed overview of the utilized instrumentation [12-17].

The standard CFR engine is equipped with a carburetor and is designed to operate at naturally aspirated conditions. Rockstroh et al. designed and implemented a compressed air intake system for the CFR engine at Argonne National Laboratory in a previous publication [18]. Figure 3 shows the CFR engine setup with the components of the compressed air intake system. Dry, oil-free, and filtered compressed air is supplied to the engine and the pressure is regulated by an Alicat mass flow controller before entering the intake

manifold 6” diameter transfer tube. The system also contains a pressure relief and a vacuum check valve to safeguard the pressure range in the manifold. Due to limitations of the standard sealing surfaces throughout the intake manifold, the intake pressure was limited to a maximum of 1.5 bara.

Table 5. Combustion research measurement and instrumentation systems installed on the CFR engine at Argonne National Laboratory.

Crankshaft angle-based measurements	
Crank-angle-based DAQ	AVL IndiCom & crankshaft encoder with 0.1 CAD resolution
Spark timing	Current clamp on coil wire
Intake pressure	Kulite flush-mounted uncooled high-speed 2.0 bara pressure transducer
Exhaust pressure	Kulite flush-mounted water-cooled high-speed 3.5 bara pressure transducer
Cylinder pressure	AVL GU13Z-24 flush-mounted spark plug pressure transducer
Time-based measurements	
Time-based DAQ	LabVIEW
Intake pressure	Setra 3550 pressure transducer
Exhaust pressure	Setra 3550 pressure transducer
Intake, mixture, exhaust, coolant, and oil temperature	K-type thermocouples
Fuel rate	Emerson CMF010M Coriolis Meter
Lambda	Bosch wide-band lambda sensor LSU 4.9
CFR knock units	Data-logged knockmeter signal

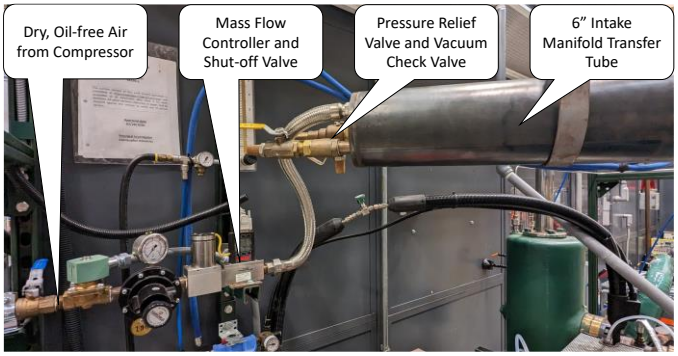

Figure 3. Compressed air intake manifold for a CFR engine.

A carburetor works based on a pressure differential in a venturi to pull fuel into the air stream. Therefore, when increasing the intake air pressure, the fuel pressure needs to match the air pressure for the carburetor to remain functional. The carburetor is retained instead of switching to a fuel injector at this stage to allow for the least amount of modifications to the CFR fueling system. Figure 4 shows a schematic of the added line routing for the carburetor (green). All conventional ventilation holes were connected to the intake manifold surge tank while the fuel bowl was sealed and also connected to the intake manifold surge tank.

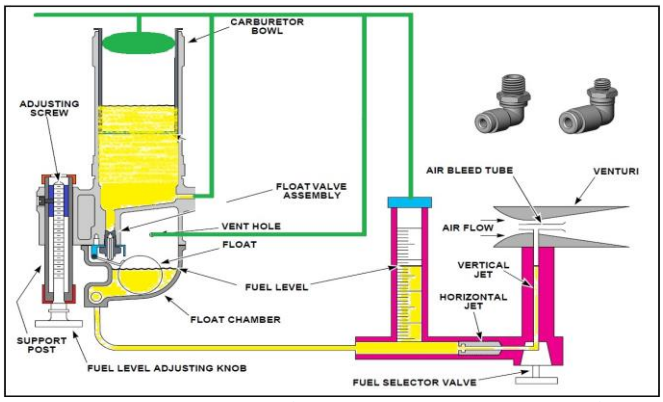

Figure 4. Carburetor line routing for operation at elevated intake and fuel pressures

The applied engine modifications did not change the geometry of the intake, exhaust, or combustion chamber. This ensured the best possible consistency with the standard CFR engine. To validate the compressed air intake system, a motored peak pressure test and a Fit for Use test following the standard ASTM D2699 RON method were conducted for multiple toluene standardization fuels (TSF) and passed the requirements without requiring temperature tuning.

Fuel Selection

This study used primary reference fuels (PRF) and toluene standardization fuels (TSF) from the standard octane test methods, along with seven full-boiling range Fuels for Advanced Combustion Engines (FACE) gasolines. During the fuel matrix design, it was important to select fuels that had a RON rating similar to each other, which coalesced around 95 RON in this study. Table 6 provides a fuel summary with octane numbers and chemical compositions. FACE B is characterized by being highly isoparaffinic, while FACE D is highly aromatic. FACE F and FACE G gasolines have olefinic (O) and cyclo-paraffinic (cP) compositions, in addition to FACE F being highly iso-paraffinic and FACE G being highly aromatic. FACE A, FACE C, and FACE H gasolines have 15 vol% ethanol. FACE A and FACE C are highly iso-paraffinic, but with minor differences in the other chemical families, while FACE H has increased levels of aromatics, cyclo-paraffins, and olefins. Three PRFs ranging from PRF 93 to PRF 97 were used as reference fuels to bracket the knocking characteristic of the gasolines. PRFs are fully paraffinic fuels and have a defined octane number equal to the volumetric concentration of iso-octane in a binary blend with n-heptane. Therefore, PRFs are defined to have a RON-MON sensitivity of 0. In addition, two TSFs with a defined composition from ASTM D2699 and RON values of 93.4 and 96.9 were used. TSFs are highly aromatic fuels and are used to ensure CFR engine compliance with the RON and MON methods.

Table 6. Overview of gasoline fuel composition and octane numbers. Chemical composition determined by detailed hydrocarbon analysis.

FACE Fuel	RON	MON	S	T90 (°F)	Iso-paraffin (vol%)	Aromatic (vol%)	N-Paraffin (vol%)	Cyclo-Paraffin (vol%)	Olefin (vol%)	Categorization	Symbol
B	95.8	92.4	3.4	236	86.9	5.8	8.0	0.1	0.02	Iso-paraffinic	
D	94.2	87.0	7.2	331	42.1	33.4	24.1	0.1	0.04	Aromatic	
F	94.0	88.1	5.9	242	67.6	7.7	4.4	11.0	9.4	Iso-paraffinic, O, cP	
G	96.5	85.8	10.7	343	38.4	33.6	6.7	11.5	8.1	Aromatic, O, cP	
A + E15	94.8	89.4	5.4	219	73.1	0.3	9.9	1.4	0.2	Iso-paraffinic, E15	
C + E15	94.8	88.8	6.0	241	59.3	3.3	20.8	0.3	1.1	Iso-paraffinic, E15	
H + E15	94.1	83.3	10.8	323	19.4	30.4	19.1	8.9	5.8	Aromatic, O, cP, E15	
PRF 93	93	93	0	-	93	0	7	0	0	Highly iso-paraffinic	
PRF 95	95	95	0	-	95	0	5	0	0	Highly iso-paraffinic	
PRF 97	97	97	0	-	97	0	3	0	0	Highly iso-paraffinic	
TSF 93.4	93.4	81.5	11.9	-	0	74	26	0	0	Highly aromatic	
TSF 96.9	96.9	85.2	11.7	-	5	74	21	0	0	Highly aromatic	

Results and Discussions

The resulting critical compression ratios from the two knock intensity thresholds are compared against each other in Figure 5. The figure also depicts a 45-degree direct correlation (gray line) as well as a linear regression line (black dashed line). Furthermore, the standard CR for RON 95 test conditions (per ASTM 2699 Procedure C) at an intake pressure of 1.0 bar and no temperature tuning are shown as red lines. Most noticeable is the negative slope of the linear regression line with a mediocre coefficient of determination of only $R^2 = 0.48$. To understand this, each axis of Figure 5 is discussed separately.

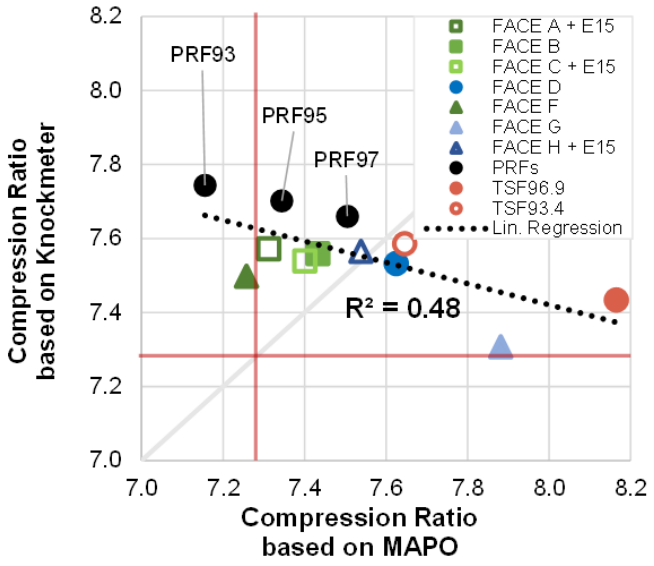

Figure 5. Comparison of variable compression ratio reactivity ratings across two knock intensity characterization techniques. The red lines mark the defined compression ratio of 7.26:1 for a standard RON95 test at 1.0 bar intake pressure.

The CR measurements for each fuel at a constant MAPO knock intensity on the x-axis followed the expected trends. The PRF97 allowed for a higher compression ratio before reaching its MAPO knock intensity threshold compared to PRF95 and PRF93, respectively. The same remained true for TSF96.9 compared to TSF93.4. A fuel chemical composition-specific trend is noticeable. Dominantly aromatic TSFs and primarily aromatic FACE gasolines (blue markers) allowed for higher compression ratios compared to primarily paraffinic FACE fuels (green markers) or purely paraffinic PRFs (black circles). Using PRF and TSF fuels, Swarts identified that highly paraffinic fuels (such as PRFs) will have higher knocking cylinder pressure oscillations than highly aromatic fuels (such as TSFs) [12]. This is consistent with findings from previous work which consistently showed higher MAPO knock intensities (at a fixed CR and spark timing) or more delayed spark timings (at a fixed KI threshold and CR) for paraffinic fuels over aromatic fuels [15,16]. As expected, FACE-G allowed the highest CR of all FACE fuels before reaching the MAPO knock intensity threshold. The 15 vol% ethanol composition of FACE A, C, and H did not have a significant effect on their MAPO-based critical CRs and the paraffinic versus aromatic composition of the based gasolines had a prevailing effect. The MAPO knock intensity metric is more relevant to knock testing in modern automotive SI engines. So, it is important to point out that now with a third test approach, fuels with similar RON rating will have a higher knock propensity when more paraffinic and lower knock propensity when higher in aromatic composition.

The CR measurements for each fuel at a constant knockmeter knock intensity on the y-axis of Figure 5 contradicted the expected trend. For PRFs with increasing RON, the knock-limited compression ratio decreased. This was also confirmed by TSF93.4, which allowed for a higher CR compared to TSF96.9. Meanwhile, all FACE fuels except for FACE-G rated close to each other. The rating behavior of the FACE-fuels can be explained by their relatively similar knockmeter knock intensities during standard RON ratings, and subsequently close RON numbers around RON95. Only FACE-G had a slightly increased RON of 96.5 (Table 6). On the contrary to the FACE fuels, PRFs and TSFs had widely varying RON numbers and ranged in their knockmeter KI based critical CRs. Previous work on the effects of lambda showed that the knockmeter knock intensity of a fuel with a lower RON and subsequently higher knock intensity had a higher knock intensity reduction when shifting operation from peak

knocking lambda to stoichiometry [12,15]. This increased change in knock intensity allowed for an exaggerated critical CR increase for fuels with lower RON subsequently leading to a higher critical CR to reach the knockmeter knock intensity threshold at stoichiometric conditions. It is emphasized that this test method, while similarly used the knockmeter like the standard Procedure C of the ASTM RON test method, differed by operating at stoichiometry and with constant combustion phasing [3]. Therefore, this test method incorporates the lambda sensitivity of a fuel into this critical compression ratio method, which surprisingly caused fuels with higher RON ratings to allow for less critical CR than fuels with lower RON. Since this is counterintuitive and not applicable to identifying knock thresholds of fuels in modern engines, further analysis of the knockmeter-based critical compression ratio results will not be further explored, and the remaining discussion will focus on the MAPO-based critical CR results.

Additional results from the MAPO-based critical CR testing are summarized in Table 7. Included are the critical CR as an indicator of fuel knock resistance, the resulting maximum pressure rise rate during testing, and the required spark timing to achieve a constant CA50 of 12 °aTDC. Furthermore, the chemical classification into paraffinic and aromatic fuels is summarized in Table 7. Primarily aromatic fuels, as also depicted on the abscissa of Figure 5, allowed for higher compression ratios compared to primarily paraffinic fuels. Furthermore, there was a noticeable increase in the maximum pressure rise rate at the knock-limited critical CR for aromatic fuels compared to paraffinic fuels. Interestingly, there was a trend of lower pressure rise rates for PRFs as their octane number increased, whereas the maximum pressure rise rates of the two TSFs were very similar. It is not clear from this work what the explanation for the varying maximum pressure rise rates might be with the different PRFs. As previously discussed, aromatic fuels tend towards higher maximum pressure rise rates, while paraffinic fuels have higher MAPO knock intensities at a given RON level. The compression ratio at the knock limit was assessed at a fixed CA50 of 12 °aTDC for each fuel. Subsequently, the spark timing was adjusted accordingly for each fuel. All three PRFs had a similar spark timing, likely because they have similar chemical composition and flame speed. Paraffinic fuels required an earlier spark timing set point than the highly aromatic fuels, suggesting a faster flame propagation for aromatic fuels. This is in line with the findings of a previous study on a modern automotive SI single-cylinder research engine, in which the measured combustion duration of toluene outperformed its flame speed [19].

Table 7. Overview of testing results for the MAPO-based variable compression ratio tests. E15 represents 15 vol% ethanol.

Fuel	Chemical Classification	CR for MAPO Threshold	Maximum Pressure Rise Rate [bar/°CA]	Spark Timing [°aTDC]
FACE-B	Paraffinic	7.43	5.9	-12.5
FACE-D	Aromatic	7.63	9.9	-10.7
FACE-F	Paraffinic	7.26	7.1	-11.7
FACE-G	Aromatic	7.88	9.9	-10.6
FACE-A +E15	Paraffinic +E15	7.31	6.6	-12.3
FACE-C +E15	Paraffinic +E15	7.40	7.3	-12.0
FACE-H +E15	Aromatic +E15	7.54	9.2	-10.1
PRF93	All paraffinic	7.16	6.2	-13.5
PRF95	All paraffinic	7.34	5.2	-13.2
PRF97	All paraffinic	7.50	3.9	-13.4
TSF93.4	Aromatic	7.65	9.9	-9.1
TSF96.9	Aromatic	8.17	9.8	-9.5

Figure 6 depicts the correlation of variable compression ratio reactivity ratings based on the MAPO knock intensity threshold to the fuel's standard RON ratings, while Figure 7 to Octane Index. The coefficient of determination suggests a mediocre correlation between the fuels' standard RON and critical CR ratings. Paraffinic fuels (green and black markers) had consistently lower compression ratios compared to aromatic fuels (blue and red markers). This trend was expected since previous work showed paraffinic fuels to suffer from higher MAPO knock intensity, subsequently reducing their knock-limited compression ratio here for a given RON rating [12,15]. It is interesting to note that the paraffinic fuels line up on a unique regression line, while the aromatic fuels had a bit more scatter. For the correlation to Octane Index, the engine operation-specific K-factor was varied to optimize the coefficient of determination. This resulted in a good correlation between the MAPO knock-limited compression ratio and Octane Index for a K-factor of -0.3, greatly improved relative to the standard RON ratings correlation (Figure 6). Based on the Octane Index theory, the slightly negative K-value suggests that the modifications to the RON test method (stoichiometry, MAPO, etc.) have led to conditions that are representative of a RON test at a lower cylinder temperature for a given cylinder pressure (aka, "beyond RON"). While the use of Octane Index as an octane metric helped to improve the correlation to the MAPO threshold knock-limited compression ratios, some fuel composition effects are still observed. For instance, the highly paraffinic FACE gasolines (A, B, C, and F) can be found at relatively lower critical CRs than the highly aromatic fuels. This aspect was consistent with Figure 6.

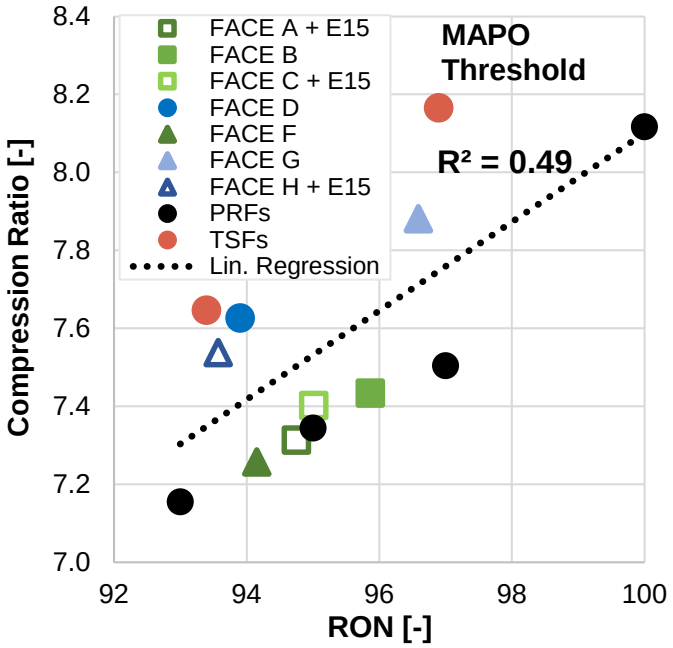

Figure 6. Comparison of critical compression ratio knock resistance ratings to standard RON ratings of the test fuels.

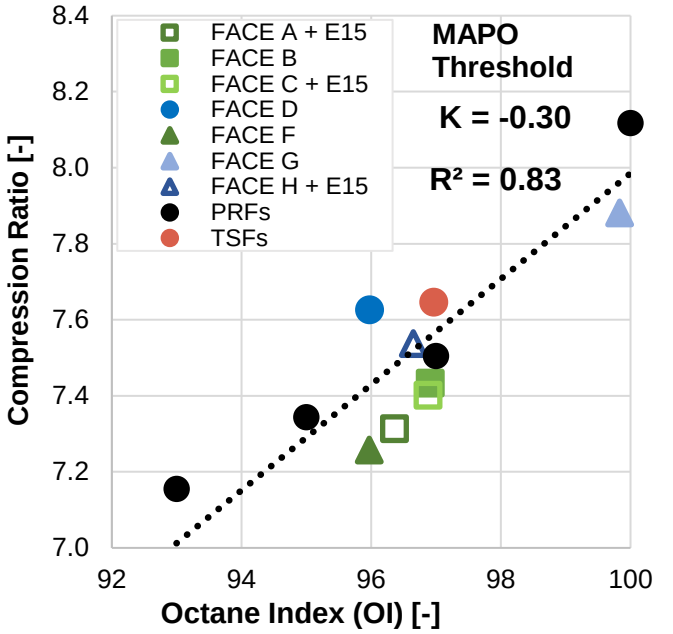

Figure 7. Comparison of critical compression ratio knock resistance ratings to Octane Index with optimized K-value for the best correlation.

Outlook and Future Work

If there would be the opportunity to further expand the scope of this work, it would be of interest to compare the critical CR knock resistance measurements explored in this study to knock-limited spark advance (KLSA) measurements of the same fuels on a modern SI engine at various knock-limited engine operating conditions, varied by speed, load, and intake conditions. Furthermore, it would be of high value to correlate the KLSA measurements from the modern SI engine to standard RON ratings, Octane Index, and the various test methods explored across this and multiple previous publications of this work [15,16].

At the time of testing, the CFR engine at Argonne National Laboratory was limited to the 600 RPM or 900 RPM engine speeds of the RON and MON tests, respectively. However, recent updates to the CFR engine test platform at Argonne National Laboratory have allowed for continuously variable engine speed up to 1,800 RPM and it would be of high value to understand how engine speed affects the observed effects of knock resistance rating method and fuel chemical composition.

In this study, the knock intensity ratings from the knockmeter pickup were based on the standard signal conditioning unit. However, recent work has shown that the standard knockmeter pickup may be capable of detecting higher frequency pressure oscillations than what is detected currently because of signal conditioning [20, 21]. It would be of interest to repeat these measurements with a MAPO-like knock intensity measurement based on the signal directly from the knockmeter pickup.

Summary and Conclusions

This work adds to the evidence that at similar conditions (CR, stoichiometry, or spark timing), knock resistance ratings by cylinder pressure based maximum amplitude of pressure oscillation (MAPO) knock intensity differs significantly from knock intensities of the standard knockmeter. The researchers propose that rating fuels at stoichiometric conditions (as opposed to the peak knock lambda approach) and rating knock intensity by a cylinder pressure-based metric, like MAPO, would be more representative to how modern SI engines operate. This work in particular detailed how critical compression ratio, similar to ASTM D2699 Procedure C, could be used as a fuel knock resistance rating metric at stoichiometric conditions with fixed CA50 combustion phasing by varying spark timing. These modifications to Procedure C would allow for air-fuel ratios and knock characterization techniques that are more relevant to modern SI engine operation and knock detection techniques.

References

1. Department of Transportation, National Highway Traffic Safety Administration, “Corporate Average Fuel Economy Standards for Model Years 2024-2026 Passenger Cars and Light Trucks”, 49 CFR Parts 523, 531, 533, 536, and 537, 2022.
2. European Parliament, “Setting CO2 emissions performance standards for new passenger cars and for new light commercial vehicles, and repealing regulations (EC) No 443/2009 and (EU) No 510/2011”, Regulation (EU) 2019-631, 2019.
3. ASTM D2699-22, “Standard Test Method for Research Octane Number of Spark-Ignition Engine Fuel,” ASTM International, West Conshohocken, PA, 2022, doi: 10.1520/D2699-22.
4. ASTM D2700-22a, “Standard Test Method for Motor Octane Number of Spark-Ignition Engine Fuel,” ASTM International, West Conshohocken, PA, 2016, doi: 10.1520/D2700-22a
5. Bartholomew, E., "NEW KNOCK-TESTING METHODS NEEDED TO MATCH ENGINE AND FUEL PROGRESS," SAE Technical Paper 610200, 1961, https://doi.org/10.4271/610200.
6. Trimble, H., “Report on the Development of the Antiknock Scale Above 100 Octane Number (1930-1958)”, ATM International Committee D02 on Petroleum Products and Lubricants, 1978.

7. Swarts, A., Yates, A., Viljoen, C., and Coetzer, R., "A Further Study of Inconsistencies between Autoignition and Knock Intensity in the CFR Octane Rating Engine," SAE Technical Paper 2005-01-2081, 2005, https://doi.org/10.4271/2005-01-2081.
8. Mittal, V., “A study of the Physics and Chemistry of Knock in Modern I Engines and Their Relationship to the Octane Tests”, Dissertation Massachusetts Institute of Technology, 2009.
9. Mittal, V. and Heywood, J., "The Shift in Relevance of Fuel RON and MON to Knock Onset in Modern SI Engines Over the Last 70 Years," SAE Int. J. Engines 2(2):1-10, 2010, doi:10.4271/2009-01-2622.
10. Kalghatgi, G., "Fuel Anti-Knock Quality- Part II. Vehicle Studies - How Relevant is Motor Octane Number (MON) in Modern Engines?," SAE Technical Paper 2001-01-3585, 2001, doi:10.4271/2001-01-3585.
11. Mittal, V. and Heywood, J., "The Relevance of Fuel RON and MON to Knock Onset in Modern SI Engines," SAE Technical Paper 2008-01-2414, 2008, doi:10.4271/2008-01-2414.
12. Swarts, A., Yates, A., Viljoen, C., and Coetzer, R., "A Further Study of Inconsistencies between Autoignition and Knock Intensity in the CFR Octane Rating Engine," SAE Technical Paper 2005-01-2081, 2005, https://doi.org/10.4271/2005-01-2081.
13. Hauber, J., Huber, K., and Nell, R., "New GKI - Gasoline Knock Index for Rating of Fuel’s Knock Resistance on an Upgraded CFR Test Engine," SAE Technical Paper 2018-01-1743, 2018, https://doi.org/10.4271/2018-01-1743.
14. Hoth, A., Pulpeiro Gonzalez, J., Kolodziej, C., and Rockstroh, T., "Effects of Lambda on Knocking Characteristics and RON Rating," SAE Int. J. Adv. & Curr. Prac. in Mobility 1(3):1188-1201, 2019, https://doi.org/10.4271/2019-01-0627.
15. Hoth, A., Kolodziej, C., “Effects of Knock Intensity Measurement Technique and Fuel Chemical Composition on the Research Octane Number (RON) of FACE Gasolines: Part 1 – Lambda and Knock Characterization”, Fuel, Volume 304, 2021, https://doi.org/10.1016/j.fuel.2021.120722.
16. Hoth, A., Kolodziej, C., “Effects of Knock Intensity Measurement Technique and Fuel Chemical Composition on the Research Octane Number (RON) of FACE Gasolines: Part 2 – Effects of Spark Timing”, Fuel, Volume 342, 2023, https://doi.org/10.1016/j.fuel.2023.127694.
17. Hoth, A., Kolodziej, C., Rockstroh, T., and Wallner, T., "Combustion Characteristics of PRF and TSF Ethanol Blends with RON 98 in an Instrumented CFR Engine," SAE Technical Paper 2018-01-1672, 2018, https://doi.org/10.4271/2018-01-1672.
18. Rockstroh, T., Kolodziej, C., Jespersen, M., Goldsborough, S. et al., "Insights into Engine Knock: Comparison of Knock Metrics across Ranges of Intake Temperature and Pressure in the CFR Engine," *SAE Int. J. Fuels Lubr.* 11(4):545-561, 2018, https://doi.org/10.4271/2018-01-0210.
19. Kolodziej, C., Pamminger, M., Sevik, J., Wallner, T. et al., "Effects of Fuel Laminar Flame Speed Compared to Engine Tumble Ratio, Ignition Energy, and Injection Strategy on Lean and EGR Dilute Spark Ignition Combustion," SAE Int. J. Fuels Lubr. 10(1):2017, doi:10.4271/2017-01-0671.
20. Swarts, A., Anderson, G., and Wallace, J., "Comparing Knock between the CFR Engine and a Single Cylinder Research Engine," SAE Technical Paper 2019-01-2156, 2019, https://doi.org/10.4271/2019-01-2156.
21. Hoth, A., “Investigation of Operational Parameter Differences between the Standard RON Test Method and Knock-Ignition Engine Operation,” PhD Thesis, Michigan Technological University, 2023.
22. Hauber, J., Huber, K., and Nell, R., “New GKI - Gasoline Knock Index for Rating of Fuel’s Knock Resistance on an Upgraded CFR Test Engine,” SAE Technical Paper 2018-01-1743, 2018, doi:10.4271/2018-01-1743.

Contact Information

Christopher P. Kolodziej, ckolodziej@anl.gov

Acknowledgments

The authors would like to thank the Coordinating Research Council (CRC) task group Advanced Vehicle Fuel Lubricants AVFL-32 for providing the FACE fuels, funding, and project guidance.

The authors would also like to acknowledge the support and contribution of Dr. Scott Miers as PhD advisor of Alexander Hoth and thank Timothy Rutter for his technical support.

Argonne is a U.S. Department of Energy laboratory managed by UChicago Argonne, LLC under contract DE-AC02-06CH11357.

Abbreviations

AKI	Anti-Knock Index
CAD	Crank Angle Degree
CFR	Cooperative Fuel Research
CR	Compression Raio
GDI	Gasoline Direct Injection
IMEP	Indicated Mean Effective Pressure
KLCA50	Knock-Limited combustion phasing for 50% mass fraction burned
KLSA	Knock-Limited Spark Advance
MAPO	Maximum Amplitude of Pressure Oscillations
MON	Motor Octane Number
NTC	Negative Temperature Coefficient
OI	Octane Index
OIs	Supercharged Octane Index
PRF	Primary Reference Fuel
R^2	Coefficient of Determination
RON	Research Octane Number
RPM	Revolutions per Minute
SI	Spark Ignition

SON	Supercharged Octane Number	**TEL**	Tetraethyl Lead
ST	Spark timing	**TSF**	Toluene Standardization Fuel